

UNIVERSIDADE DE SÃO PAULO

INSTITUTO DE FÍSICA  
CAIXA POSTAL 20516  
01498 - SÃO PAULO - SP  
BRASIL

publicação

IFUSP/P 452  
B.I.F. - USP

IFUSP/P-452



PHENOMENOLOGICAL RENORMALIZATION GROUP CALCULATIONS  
FOR 12- AND 16-VERTEX MODELS ON A SQUARE LATTICE

by

J.F. Stilck, M.J. de Oliveira, and S.R. Salinas  
Instituto de Física, Universidade de São Paulo

Fevereiro/1984

PHENOMENOLOGICAL RENORMALIZATION GROUP CALCULATIONS  
FOR 12- AND 16-VERTEX MODELS ON A SQUARE LATTICE

J.F. Stilck, M.J. de Oliveira, and S.R. Salinas  
Instituto de Física, Universidade de São Paulo  
C.P. 20516, 01498 São Paulo, SP, Brazil

ABSTRACT

We performed phenomenological renormalization group calculations for ferroelectric 12- and 16-vertex models on a square lattice with periodic and helical boundary conditions. We considered strips of infinite length and finite widths ( $n=1$  to 7, 8 or 9). The extrapolated values for the transition temperature of the 12-vertex model, which has been used for assessing the transition in squaric acid, are lower than the predictions of the Bethe approximation. The estimates for the critical exponent  $\nu$  do not allow a definite conclusion about its asymptotic behavior, although the Ising value  $\nu=1$  seems more plausible. The estimates for the 16-vertex model considered in this paper, which is equivalent to an anisotropic nearest-neighbor Ising model, show an excellent convergence to the exact values. Also, we analyze the finite size scaling behavior of the critical free energy of both models.

I. INTRODUCTION

The so-called phenomenological renormalization group, proposed by Nightingale a few years ago<sup>(1)</sup>, proved to be a powerful method for studying the critical behavior of two-dimensional model systems<sup>(2)</sup>. In the present article we report phenomenological renormalization group calculations for two vertex models on a square lattice.

We first consider a 12-vertex model associated with the study of the antiferroelectric phase transition in layered hydrogen bonded crystals of squaric acid<sup>(6)</sup>. At low temperatures, the crystals of squaric acid show an antiferroelectric stacking of ferroelectrically ordered layers<sup>(4)</sup>. A ferroelectric 12-vertex model has then been shown to be adequate to account for the ordering in the layers. Although 6- and symmetrical 8-vertex models on a square lattice can be solved exactly, the 12-vertex model does not seem amenable to an exact treatment. On the other hand, in a Bethe cluster approximation, which gives reasonable results for 6- and 8-vertex models, we have shown the occurrence of a continuous phase transition. It is thus of interest to use more powerful methods to investigate the critical behavior of the 12-vertex model, and to check the predictions of the cluster approximation.

The techniques we use are suitable for assessing the critical behavior of more general vertex models on a square lattice. So, we decided to investigate the critical properties

of a certain 16-vertex model, which is isomorphous to an Ising model with anisotropic first neighbor interactions. Since the critical singularities of this Ising model are known exactly, the calculations reported in the present paper are a good test for the reliability of the method. In particular, we reproduce, with a somewhat better accuracy, earlier phenomenological renormalization group results for the anisotropic Ising model.

In section II we define the 12- and 16-vertex models considered in this article. Also, we briefly review the equivalence between a 16-vertex model on a square lattice and an anisotropic Ising model with first and second neighbor interactions and four-spin terms. It should be noted that the existence of a phase transition in the ferroelectric 12-vertex model on a square lattice may be established by the application of a Peierls argument<sup>(5)</sup>. In section III we recall a theorem by Suzuki and Fisher<sup>(6)</sup> concerning the behavior of the zeros of the partition function for vertex models in the complex electric field plane. Arguments based on this theorem indicate that the Bethe approximation may be giving an overestimated value for the critical temperature. This has been confirmed by our renormalization group calculations for the 12-vertex model.

The numerical estimates for the values of the critical temperature and the exponent  $\nu$  are given in section IV. The results for the 16-vertex model show an excellent convergence. The convergence of the estimates for the exponent  $\nu$  of the 12-vertex model are much poorer, although the Ising

value  $\nu=1$  seems indeed more plausible. Some finite size scaling data for the critical free energy of these models are analyzed in section V. For the 16-vertex model they exhibit the expected behavior. However, for the 12-vertex model it seems that corrections to scaling are still important even at the highest orders (strips of widths  $n=8$  and  $9$ ) we were able to consider. A summary and some conclusions are presented in section VI.

## II. DEFINITION OF THE MODELS

The vertex configurations of the 16-vertex model may be numbered as shown in Fig. 1. We will be concerned with arrow inversion invariant energy levels,  $e_{\xi}$ , given by

$$\begin{aligned} e_1 = e_2 = E_1 ; e_3 = e_4 = E_2 ; e_5 = e_6 = E_3 ; \\ e_7 = e_8 = E_4 ; e_9 = e_{13} = E_5 ; e_{10} = e_{14} = E_6 ; \\ e_{11} = e_{15} = E_7 ; e_{12} = e_{16} = E_8 . \end{aligned} \quad (2.1)$$

This vertex model can be converted into an Ising model with first-neighbor, second-neighbor and four-spin interactions<sup>(6)</sup>. Let us define Ising-like variables  $\sigma_l$  on the links of the original lattice, such that  $\sigma_l = \pm 1$ , if the arrow on the link

points up or rightwards, and  $\sigma_i = -1$ , if it points down or leftwards. The energy of each vertex may then be written as a function of the four incident Ising spins (see Fig. 2).

Therefore, we have

$$E(\sigma_1, \sigma_2, \sigma_3, \sigma_4) = -J_0 - (J_1\sigma_1\sigma_2 + J_2\sigma_2\sigma_3 + J_3\sigma_3\sigma_4 + J_4\sigma_4\sigma_1) - (J_5\sigma_1\sigma_3 + J_6\sigma_2\sigma_4) - J_7\sigma_1\sigma_2\sigma_3\sigma_4, \quad (2.2)$$

where

$$J_0 = -\frac{1}{8} \sum_{i=1}^8 E_i, \quad (2.3a)$$

$$J_1 = \frac{1}{8} (E_2 + E_3 + E_7 + E_8) + (E_1 + E_4 + E_5 + E_6), \quad (2.3b)$$

$$J_2 = \frac{1}{8} (E_2 + E_4 + E_5 + E_8) - (E_1 + E_3 + E_6 + E_7), \quad (2.3c)$$

$$J_3 = \frac{1}{8} (E_2 + E_3 + E_5 + E_6) - (E_1 + E_4 + E_7 + E_8), \quad (2.3d)$$

$$J_4 = \frac{1}{8} (E_2 + E_4 + E_6 + E_7) - (E_1 + E_3 + E_5 + E_8), \quad (2.3e)$$

$$J_5 = \frac{1}{8} (E_3 + E_4 + E_5 + E_7) - (E_1 + E_2 + E_6 + E_8), \quad (2.3f)$$

$$J_6 = \frac{1}{8} (E_3 + E_4 + E_6 + E_8) - (E_1 + E_2 + E_5 + E_7), \quad (2.3g)$$

$$J_7 = \frac{1}{8} (E_5 + E_6 + E_7 + E_8) - (E_1 + E_2 + E_3 + E_4). \quad (2.3h)$$

With the particular choice

$$E_1 = -2J(1+R) ; E_2 = 2J(1+R), \quad (2.4a)$$

$$E_3 = 2J(1-R) ; E_4 = -2J(1-R), \quad (2.4b)$$

$$E_5 = E_6 = E_7 = E_8 = 0, \quad (2.4c)$$

the 16-vertex model corresponds to an anisotropic Ising model with interactions  $J_1 = J_3 = J$  and  $J_2 = J_4 = RJ$  between nearest neighbors only. The exact critical temperature of this model is given by<sup>(7)</sup>

$$\cosh\left(\frac{2J}{kT_c}\right) \cosh\left(\frac{2RJ}{kT_c}\right) = \sinh\left(\frac{2J}{kT_c}\right) + \sinh\left(\frac{2RJ}{kT_c}\right), \quad (2.5)$$

and the correlation length critical exponent is  $\nu = 1$ <sup>(8)</sup>.

The ferroelectric 12-vertex model<sup>(3)</sup> is defined by the energy levels

$$E_1 = 0 ; E_2 = E > 0 ; E_5 = E_6 = E_7 = E_8 = E' > 0 ; E_3, E_4 \rightarrow \infty. \quad (2.6)$$

In the Bethe approximation, it exhibits a ferroelectric phase transition of second order<sup>(3)</sup>. Using a rigorous version of the Peierls argument, provided that  $E, E' > 0$ , it is possible to confirm the existence of this phase transition<sup>(5)</sup>.

### III. BEHAVIOR OF THE ZEROS OF THE PARTITION FUNCTION

Consider ferroelectric vertex models with the lowest energy levels defined by  $e_1 = e_2 = E_1$ . A theorem proved by Suzuki and Fisher<sup>(6)</sup> asserts that the zeros of the partition function lie on a unit circle in a complex  $e^{-\beta\epsilon}$ -plane, where  $\epsilon$  is the ordering electric field, provided that the condition

$$e^{-\frac{E_1}{kT}} \geq \sum_{j=2}^8 e^{-\frac{E_j}{kT}} \quad (2.7)$$

is fulfilled. There is thus a limiting temperature  $T_0$  for which the inequality (2.7) turns into an equality. Below  $T_0$  the unit circle theorem holds for these vertex models.

For a ferroelectric 6-vertex model ( $E_1 = 0$ ;  $E_2 = E_3 = E > 0$ ;  $E_4, E_5, E_6, E_7, E_8 \rightarrow \infty$ ), as well as an 8-vertex model ( $E_1 = 0$ ;  $E_2 = E_3 = E > 0$ ;  $E_4 = E' > 0$ ;  $E_5, E_6, E_7, E_8 \rightarrow \infty$ ), whose exact solutions are known<sup>(8)</sup>, the limiting temperature  $T_0$  coincides with the transition temperature. Numerical calculations for finite 6-vertex models seem to indicate that the zeros of the partition function actually get off the unit circle for temperatures above  $T_0$ <sup>(9)</sup>. On the other hand, the zeros of the partition function for the 16-vertex model (2.4) are known to lie on the unit circle at all temperatures<sup>(10)</sup>. In this case the limiting temperature  $T_0$  has no special meaning.

There is also a peculiar coincidence between the exact transition temperature,  $T_c$ , of the 6- and 8-vertex models

defined above and the corresponding temperatures,  $T_{c,B}$ , predicted by the Bethe approximation. Since  $T_{c,B} > T_0$  for the 12-vertex model, we suspected that the Bethe approximation overestimates the critical temperature. The renormalization group calculations presented in this paper were undertaken in part to clear up this point.

### IV. RENORMALIZATION GROUP CALCULATIONS

We considered vertex models defined on strips of infinite length and finite width (geometry B, as called by Brézin<sup>(11)</sup>). The correlation lengths in the longitudinal direction were calculated by a transfer matrix formalism. The renormalization of the temperature was then obtained via the scaling relation for the correlation length<sup>(1,11)</sup>,

$$\frac{\xi_n(z)}{\xi_{n-1}(z')} = \frac{n}{n-1} \quad (3.1)$$

where  $z$  is an activity, and we choose pairs of strips with widths  $n$  and  $n-1$ . The fixed point of the recurrence relation  $z' = z'(z)$  gives estimates for the critical activity  $z_c$ ,

$$\frac{\xi_n(z_{c,n})}{\xi_{n-1}(z_{c,n})} = \frac{n}{n-1} \quad (3.2)$$

Estimates for the exponent  $\nu$  may be calculated by a linearization of the recurrence relation in the neighborhood of the fixed point. We thus have

$$\nu_n = \left\{ \frac{\ln[\xi_n(z_{C,n})/\xi_{n-1}(z_{C,n})]}{\ln[n/(n-1)]} - 1 \right\}, \quad (3.3)$$

where  $\xi \equiv \frac{d\xi}{dz}$ .

Two sequences of estimates were obtained: (i) for periodic boundary conditions, and with the usual definition of the transfer matrix for vertex models<sup>(12)</sup>; (ii) for helical boundary conditions. Details regarding the definitions and calculation of the transfer matrices, as well as the determination of the correlation lengths, are given in the Appendices. In general, the transfer matrices of vertex models with periodic boundary conditions are not hermitian. However, it is remarkable that the ferroelectric 12-vertex model obeys the conditions  $E_3 = E_4$  and  $E_5 = E_7$ , which are enough for assuring that the corresponding transfer matrix is hermitian.

In Table 1 we display estimates of  $z_C = \exp(-E/kT_C)$  and the exponent  $\nu$  for the 12-vertex model with periodic boundary conditions, for six different values of the ratio  $p = E/E'$ . In the limit  $p \rightarrow 0$ , the 12-vertex model reduces to a 4-vertex model, and  $z_C = 1$ <sup>(3)</sup>. The values of  $z_{C,B} = \exp(-E/kT_{C,B})$ , corresponding to the Bethe approximation, and of  $z_0 = \exp(-E/kT_0)$  are also given in Table 1. It is apparent that, in general,

$T_0 < T_C < T_{C,B}$  for the 12-vertex model. Estimates for this model submitted to helical boundary conditions are shown in Table 2. In Figs. (3a) and (3b) the estimates for the 12-vertex model are displayed graphically.

The estimates for the 16-vertex model, which is equivalent to an anisotropic Ising model, are given in Tables 3 and 4, for periodic and helical boundary conditions respectively. These estimates, as well as the exact values of  $z_C = \exp(-J/kT_C)$  and  $\nu$ , are plotted in Figs. (4a) and (4b).

The estimates for the 16-vertex model converge to their asymptotic values faster than the corresponding ones for the 12-vertex model. As a matter of fact, for the 12-vertex model, the curves  $z_{C,n} \times n$  and  $\nu_n \times n$  display in some cases a non-monotonic behavior. We thus conclude that the estimates for the 12-vertex model, up to the orders we considered, have not reached the regime where their convergence is governed by the leading irrelevant-variable scaling exponent<sup>(13)</sup>. This makes it difficult to devise a reliable extrapolation scheme for the estimates, particularly for those of the exponent  $\nu$ . Therefore, it remains an open question whether  $\nu$  has a unique value for the 12-vertex model. We recall that calculations for the 8-vertex model indicate that the phenomenological renormalization group technique may give good results for systems with nonuniversal critical behavior<sup>(14)</sup>. Nevertheless, some fits of our estimates for the 12-vertex model, with the allowance of logarithmic corrections, are consistent with the

assumption that it has a universal critical behavior, with  $\nu=1$ . These fits, however, are by no means definitive.

The estimates for the 16-vertex model behave as expected. In Table 5 we present results of 3-point fits of functions of the form  $A + Bn^{-x}$  to the estimates. They seem to be consistent with  $x_z = 3$  for  $z_{c,n}$  and  $x_\nu = 2$  for  $\nu_n$ . This supports the scaling relation<sup>(13,15)</sup>

$$x_z - x_\nu = 1/\nu \quad (3.4)$$

The exponents governing the convergence of our estimates seem to be given by the usual values obtained in the Onsager formulation of the Ising model<sup>(15)</sup>. The amplitudes, however, are different. Our estimates converge more rapidly to their asymptotic values than the corresponding ones obtained via the Onsager formulation of the transfer matrix<sup>(1,16)</sup>. Also, due to the way we formulate the Ising model, even in the anisotropic case ( $R \neq 1$ ), the direction in which the correlation length is calculated is equivalent to the direction along which the widths of the strips are measured.

#### IV. FINITE SIZE SCALING OF THE FREE ENERGY

According to finite size scaling arguments, the critical free energy per vertex is asymptotically given by

$$f_n \approx A + Bn^{-d} \quad (4.1)$$

where  $d$  is the spatial dimensionality of the lattice<sup>(17)</sup>. In order to verify Eq. (4.1), we calculated the critical free energies,  $f_n$ , given by

$$f_n = -kT_c \frac{\ln Z_n(T_c)}{NJ} \quad (4.2)$$

for the 16-vertex Ising model with strips of width  $n$  (for the 12-vertex model  $J$  should be replaced by  $E$ ).

In Table 6 we give values of the critical free energy  $f_n$  for Ising models with width  $n$  and periodic boundary conditions. Three point fits of functions of the form  $A + Bn^{-x}$  to these values seem to support the prediction  $x = 2$  (see Table 7). In these calculations, the values of  $f_n$  converge faster than in the usual Onsager formulation of the Ising model. For the isotropic case,  $B \approx 1.188142$  in the Onsager formulation, whereas  $B \approx 0.557$  in our calculations.

Similar calculations for the 12-vertex model are not so accurate since the exact critical temperature is not known. Values for  $f_n$  obtained using the estimates for  $z_c$  of the preceding section provided non-monotonic estimates for  $B$  and  $x$ . We are thus led to the conclusion that the asymptotic regime has not been attained and, therefore, higher order corrections to scaling become relevant.

## V. CONCLUDING REMARKS

We performed phenomenological renormalization group calculations and used finite size scaling arguments to analyze the critical behavior of 12- and 16-vertex models on a square lattice.

For a particular 16-vertex model, which is equivalent to the anisotropic Ising model with first neighbor interactions, the RG calculations produced quite accurate results both for the critical temperature and for the critical exponent  $\nu=1$ . Also, the behavior of the estimates as a function of the widths of the strips used in the calculations is well described by the expected asymptotic scaling law. It is thus possible to devise a reliable extrapolation scheme. We obtain extrapolated values with relative errors of about  $10^{-3}\%$  for  $T_c$  and  $10^{-1}\%$  for  $\nu$ . The critical free energies of the strips are also in good agreement with the expected asymptotic behavior for the 16-vertex Ising model.

The results for the ferroelectric 12-vertex model are not so well behaved. In several cases, the estimates for  $z_c$  and  $\nu$  show a nonmonotonic dependence on the width of the strips. This is an indication that the asymptotic regime has not been reached up to the widths we considered. Nevertheless, the estimates for  $z_c$  are sufficiently accurate to allow the conclusion that the Bethe approximation for the 12-vertex model leads to an overestimated value of the critical temperature.

Although we believe that the correlation length exponent for the 12-vertex model is equal to the Ising value,  $\nu=1$ , other values of  $\nu$ , or even a nonuniversal behavior of the model, cannot be ruled out by our estimates.

All calculations were performed for vertex models defined on strips of widths up to  $n=7$  (16-vertex model with periodic boundary conditions),  $n=8$  (12-vertex model with periodic boundary conditions), and  $n=9$  (helical boundary conditions). We believe that it would be feasible to consider larger strips, particularly in the case of helical boundary conditions, and to use better numerical methods for obtaining the two largest eigenvalues of the transfer matrix (we used a variation of the power method<sup>(18)</sup>). Nevertheless, since the estimates seem to converge slowly, it is doubtful whether this improvement would provide a definitive answer about the value of the critical exponent  $\nu$  for the 12-vertex model.

## ACKNOWLEDGMENTS

We acknowledge the financial support of the Brazilian agencies CNPq and FINEP.



APPENDIX 1 - TRANSFER MATRIX FOR VERTEX MODELS WITH HELICAL BOUNDARY CONDITIONS

Consider a vertex model defined on a strip of width  $n$  and length  $m$ . The total number of vertices will be  $N = nm$ . Usually<sup>(12)</sup>, the transfer matrix with periodic boundary conditions is defined by

$$T(\phi, \phi') = \sum_{\theta} \exp \left[ - \frac{E_n(\phi, \theta, \phi')}{kT} \right], \quad (A1.1)$$

where  $\phi$  and  $\phi'$  label the configurations of two disjoint sets of  $n$  vertical bonds, and  $\theta$  labels the configuration of the  $n$  horizontal bonds between them (see Fig. 5). The value of  $E_n(\phi, \theta, \phi')$  is given by the sum of the contributions of the  $n$  vertices whose configurations are defined by  $\phi$ ,  $\theta$  and  $\phi'$ . In the limit  $m \rightarrow \infty$ , the partition function is asymptotically given by

$$Z_{nm} \approx \lambda_1^m, \quad (A1.2)$$

where  $\lambda_1$  is the largest eigenvalue of the matrix  $T(\phi, \phi')$ . Also, the correlation length associated with the vertical bond-vertical bond correlations in the longitudinal direction is given by

$$\xi = \left[ \ln \left( \frac{\lambda_1}{\lambda_2} \right) \right]^{-1}, \quad (A1.3)$$

where  $\lambda_2$  is the second largest eigenvalue. Alternatively, we may define the vertex model on a strip where the horizontal bonds lay along a helix. These boundary conditions were used by Kramers and Wannier for the Ising model<sup>(19)</sup>. We may then number the vertices, as well as the vertical and horizontal bonds, along the helix, as depicted in Fig. 6, and associate an Ising spin  $\sigma_v(\sigma_n)$  with each vertical (horizontal) bond according to the conventions of section II. The hamiltonian may then be written as

$$H = \sum_{i=1}^N E(\sigma_{v_i}, \sigma_{h_{i-1}}, \sigma_{v_{i-n}}, \sigma_{h_i}), \quad (A1.4)$$

with

$$\sigma_{v_0} = \sigma_{v_N}, \sigma_{v_{-1}} = \sigma_{v_{N-1}}, \dots, \sigma_{v_{1-n}} = \sigma_{v_{N-n+1}}; \quad (A1.5a)$$

and

$$\sigma_{h_0} = \sigma_{h_N}. \quad (A1.5b)$$

The partition function is given by

$$Z_n = \sum_{\{\sigma_v\}} \sum_{\{\sigma_n\}} \prod_{i=1}^N \exp \left[ - E(\sigma_{v_i}, \sigma_{h_{i-1}}, \sigma_{v_{i-n}}, \sigma_{h_i}) / kT \right]. \quad (A1.6)$$

Let us now group the bonds in  $N$  sets of  $(n+1)$  bonds defined by

$$S_i = \left\{ \sigma_{v_{i-1}}, \sigma_{v_{i-2}}, \dots, \sigma_{v_{i-n}}, \sigma_{h_{i-1}} \right\}, \quad (A1.7)$$

with  $i = 1, 2, \dots, N$ , and  $S_{N+1} = S_1$ . The configurations of each set may be labeled by an index  $\phi_i = 1, 2, \dots, 2^{N+1}$ , and the partition function (A1.6) may be rewritten as

$$Z_n = \sum_{\phi_1=1}^{2^{n+1}} \sum_{\phi_2=1}^{2^{n+1}} \dots \sum_{\phi_N=1}^{2^{n+1}} \prod_{i=1}^N T(\phi_i, \phi_{i+1}) = \text{Tr } \underline{T}^N, \quad (A1.8)$$

where

$$T(\phi_i, \phi_{i+1}) = \begin{cases} 0, & \text{if } \phi_{i+1} \text{ is not compatible } \phi_i, \\ \exp \left[ -E(v_i, h_{i-1}, v_{i-n}, h_i) / kT \right], & \text{if they are compatible.} \end{cases} \quad (A1.9)$$

It should be remarked that the transfer matrix will be sparse. There will be at most four non zero elements in each line. In the limit  $m \rightarrow \infty$ , the partition function and the correlation length will be given by

$$Z_N \approx \Lambda_1^N, \quad (A1.10)$$

and

$$\xi \approx \left[ \ln \left( \frac{\Lambda_1}{\Lambda_2} \right) \right]^{-1}, \quad (A1.11)$$

where  $\Lambda_1$  and  $\Lambda_2$  are the largest and the second largest eigenvalues of the transfer matrix respectively.

## APPENDIX 2 - BLOCK-DIAGONALIZATION OF THE TRANSFER MATRIX OF VERTEX MODELS WITH PERIODIC BOUNDARY CONDITIONS

Before performing numerical calculations with periodic boundary conditions we used symmetry properties to algebraically block-diagonalize the transfer matrix. As may be seen in Appendix 1, the states which define the transfer matrix are invariant under rotations of  $2\pi/n$ , as well as under the inversion of the arrows. Therefore, the symmetry group to be considered is  $C_{n,h} = C_n \otimes S_2$ . First, we obtained the character table of this group, with  $n$  between 2 and 8. We then constructed the unitary matrix  $\underline{S}$  in order to transform  $\underline{T}$  into  $\underline{T}' = \underline{S} \times \underline{T} \times \underline{S}^\dagger$ . The computational effort in doing these calculation grows very fast with  $n$ , and this imposed severe limitations on the widths we were able to consider.

REFERENCES

- (1) M.P. Nightingale, *Physica* 83A, 561 (1976).
- (2) P. Nightingale, *J. Appl. Phys.* 53, 7927 (1982).
- (3) J.F. Stilck and S.R. Salinas, *J. Chem. Phys.* 75, 1368 (1981).
- (4) D. Semmingsen and J. Feder, *Solid State Commun.* 15, 1369 (1974).
- (5) J.F. Stilck, *J. Phys.* A16, L629 (1983).
- (6) M. Suzuki and M.E. Fisher, *J. Math. Phys.* 13, 62 (1969).
- (7) L. Onsager, *Phys. Rev.* 65, 117 (1944).
- (8) R.J. Baxter, "Exactly Solved Models in Statistical Mechanics", Academic Press (1982).
- (9) S. Katsura, Y. Abe and K. Ohkouchi, *J. Phys. Soc. Jpn.* 29, 845 (1970).
- (10) T.D. Lee and C.N. Yang, *Phys. Rev.* 87, 410 (1952).
- (11) E. Brézin, *J. Physique* 43, 15 (1982).
- (12) E.H. Lieb and F.Y. Wu, in "Phase Transitions and Critical Phenomena", Vol. 1, ed. by C. Domb and M.S. Green, Academic Press (1972).
- (13) V. Privman and M.E. Fisher, *J. Phys.* A16, L295 (1983).
- (14) M.P. Nightingale, *Phys. Lett.* 59A, 486 (1977).
- (15) B. Derrida and L. De Sèze, *J. de Phys.* 43, 475 (1982).
- (16) L. Sneddon, *J. Phys.* C11, 2823 (1978).
- (17) H.W.J. Blöte and M.P. Nightingale, *Physica* 112A, 405 (1982).

- (18) D.K. Faddeev and V.N. Fadееva, "Computational Methods of Linear Algebra", W.H. Freeman (1963).
- (19) H.A. Kramers and G.H. Wannier, *Phys. Rev.* 60, 252 (1941).

TABLE CAPTIONS

TABLE 1 - Estimates of the critical activity  $z_c$  and the exponent  $\nu$  for the ferroelectric 12-vertex model with periodic boundary conditions. The subscript  $n$  refers to a comparison between two models with widths  $n$  and  $n-1$ . Values of  $z_{c,B} = \exp[-E/kT_{c,B}]$  and  $z_0 = \exp[-E/kT_0]$  are also given. The parameter  $p$  is given by the ratio  $E/E'$ , with the energy levels defined in Eq. (2.6).

TABLE 2 - Estimates of the critical activity  $z_c$  and the exponent  $\nu$  for the ferroelectric 12-vertex model with helical boundary conditions.

TABLE 3 - Estimates of  $z_c = \exp[-J/kT_c]$  and the exponent  $\nu$  for the particular 16-vertex model defined by Eqs. (2.4), with periodic boundary conditions.  $J$  and  $RJ$  are the exchange parameters of the equivalent anisotropic Ising model on the square lattice. The exact values of  $z_c$  and  $\nu$  are also given.

TABLE 4 - Estimates of  $z_c$  and  $\nu$  for the 16-vertex model defined by Eqs. (2.4) with helical boundary conditions.

TABLE 5 - Three-point fits for the estimates in Table 3 with functions of the form  $A + Bn^{-x}$ , associated with 3 consecutive widths,  $n, n+1$ , and  $n+2$ .

TABLE 6 - Values of the critical free energy for the 16-vertex Ising model with periodic boundary conditions.

TABLE 7 - Three-point fits with functions of the form  $A + Bn^{-x}$  for the critical free energies of Table 6.

FIGURE CAPTIONS

FIG. 1 - The 16-vertex configurations on a square lattice.

FIG. 2 - Numbering scheme for the four links incident on a vertex.

FIG. 3 - Graphs of the estimates for  $z_c$  and  $v_n$ , as a function of the widths  $n$ , of the ferroelectric 12-vertex model: (a) estimates of  $z_c$ , with periodic (pbc) and helical (hbc) boundary conditions (see Tables 1 and 2); (b) estimates of  $v_n$  with periodic boundary conditions (see Table 1) and with helical boundary conditions (see Table 2). We display results for several values of the parameter  $p = E/E'$ .

FIG. 4 - Graphs of the estimates, as a function of the widths  $n$ , for the particular 16-vertex model defined by Eqs. (2.4) (see Tables 3 and 4): (a) estimates of  $z_c$ , with periodic (pbc) and helical (hbc) boundary conditions; (b) estimates of  $v_n$ , with periodic (pbc) and helical (hbc) boundary conditions.

FIG. 5 - Two rows of vertical bonds and a row of horizontal bonds for a vertex model with periodic boundary conditions and width  $n = 4$ .

FIG. 6 - A lattice with  $n=4$  and  $m=6$  submitted to helical boundary conditions.

$p = 2$   $z_{c,B} = 0.17157$   $z_0 = 0.055728$

n	$z_{c,n}$	$v_n$
3	0.15711500	1.32281
4	0.12713754	1.03601
5	0.11242518	0.97044
6	0.10525549	0.95952
7	0.10171230	0.96418
8	0.09991605	0.97162

$p = 1$   $z_{c,B} = \frac{1}{3}$   $z_0 = 0.2$

n	$z_{c,n}$	$v_n$
3	0.28363586	1.05740
4	0.29328729	0.95892
5	0.28704290	0.92826
6	0.28013124	0.92822
7	0.27519931	0.93767
8	0.27207939	0.94861

$p = \frac{1}{2}$   $z_{c,B} = \frac{1}{2}$   $z_0 = 0.39039$

n	$z_{c,n}$	$v_n$
3	0.42472724	0.92601
4	0.45779363	0.87494
5	0.46783721	0.84634
6	0.46903156	0.84402
7	0.46740729	0.85684
8	0.46524498	0.87566

$p = \frac{1}{3}$   $z_{c,B} = 0.58975$   $z_0 = 0.5$

n	$z_{c,n}$	$v_n$
3	0.50742270	0.89502
4	0.54334948	0.84354
5	0.55938466	0.80881
6	0.56563497	0.79395
7	0.56736360	0.79627
8	0.56715959	0.80967

$p = \frac{1}{4}$   $z_{c,B} = 0.64780$   $z_0 = 0.57195$

n	$z_{c,n}$	$v_n$
3	0.56410369	0.88735
4	0.59872374	0.83059
5	0.61657382	0.79203
6	0.62536962	0.76870
7	0.62930096	0.76068
8	0.63071520	0.76489

$p = \frac{1}{5}$   $z_{c,B} = 0.68914$   $z_0 = 0.62340$

n	$z_{c,n}$	$v_n$
3	0.60625166	0.88739
4	0.63868220	0.82563
5	0.65671836	0.78448
6	0.66669694	0.75633
7	0.67197126	0.74083
8	0.67454728	0.73690

TABLE 1

p = 2

n	$z_{c,n}$	$v_n$
3	0.052959817	1.33108
4	0.078346631	1.15129
5	0.090241482	1.06366
6	0.094997287	1.02277
7	0.096751839	1.00443
8	0.097352212	0.99687
9	0.097526405	0.99314

p = 1

n	$z_{c,n}$	$v_n$
3	0.19417511	1.27706
4	0.23339737	1.11834
5	0.25204825	1.04047
6	0.26068100	1.00307
7	0.26456503	0.98657
8	0.26623155	0.97885
9	0.26692300	0.98011

p = 1/2

n	$z_{c,n}$	$v_n$
3	0.38299787	1.25108
4	0.41870541	1.10051
5	0.43664550	1.02298
6	0.44630372	0.98231
7	0.45166761	0.96122
8	0.45467562	0.95106
9	0.45636544	0.94888

p = 1/3

n	$z_{c,n}$	$v_n$
3	0.49262761	1.24906
4	0.52247557	1.09774
5	0.53779513	1.01947
6	0.54653687	0.97621
7	0.55181607	0.95162
8	0.55510245	0.93822
9	0.55718220	0.93177

p = 1/4

n	$z_{c,n}$	$v_n$
3	0.56495065	1.24484
4	0.59030387	1.09738
5	0.60344838	1.01907
6	0.61116536	0.97450
7	0.61603964	0.94982
8	0.61922218	0.93203
9	0.62135662	0.92321

p = 1/5

n	$z_{c,n}$	$v_n$
3	0.61683873	1.24517
4	0.63882430	1.09813
5	0.65028434	1.01974
6	0.65712219	0.97429
7	0.66153092	0.84615
8	0.66451919	0.92941
9	0.66659980	0.91886

TABLE 2

R = 1

$z_c = 0.64360$

v = 1

n	$z_{c,n}$	$v_n$
3	0.63969666	1.03928
4	0.64205922	1.02131
5	0.64294361	1.01329
6	0.64317412	1.00894
7	0.64333632	1.00659

R = 2

$z_c = 0.73736$

v = 1

n	$z_{c,n}$	$v_n$
3	0.73507046	1.04256
4	0.73649549	1.02562
5	0.73694490	1.01775
6	0.73712829	1.01339
7	0.73721644	1.01068

TABLE 3

R = 1

n	$z_{c,n}$	$v_n$
3	0.624858	1.06027
4	0.635628	1.03877
5	0.639540	1.02639
6	0.641271	1.01886
7	0.642147	1.01412
8	0.642634	1.01094
9	0.642926	1.00860

R = 2

n	$z_{c,n}$	$v_n$
3	0.716229	1.16008
4	0.726435	1.10592
5	0.730778	1.07725
6	0.732993	1.05993
7	0.734264	1.04841
8	0.735056	1.04032
9	0.735582	1.03452

TABLE 4

R = 1,  $z_c$

n	A	B	x
3	0.64358	-0.14020	3.2656
7	0.64359	-0.13464	3.2312
5	0.64359	-0.13062	3.2093

R = 1,  $v$

n	A	B	x
3	1.00018	0.41017	2.1395
4	0.99910	0.35904	2.0073
5	1.00192	0.80376	2.6461

R = 2,  $z_c$

n	A	B	x
3	0.73733	-0.10117	3.4600
4	0.73734	-0.09262	3.3859
5	0.73735	-0.08578	3.3309

R = 2,  $v$

n	A	B	x
3	1.00363	0.34489	1.9857
4	1.00289	0.31852	1.9042
5	1.00232	0.28928	1.8211

TABLE 5

R = 1

n	$f(0, n^{-1})$
2	-4.35935
3	-4.28347
4	-4.25584
5	-4.24283
6	-4.23571
7	-4.23139

R = 2

n	$f(0, n^{-1})$
2	-6.48424
3	-6.38193
4	-6.34500
5	-6.43769
6	-6.31823
7	-6.31250

TABLE 6

R = 1

n	A	B	x
2	-4.21759	-0.52539	1.8899
3	-4.21872	-0.54208	1.9342
4	-4.21917	-0.55794	1.9637
5	-4.21917	-0.55762	1.9633

R = 2

n	A	B	x
2	-6.29473	-0.71442	1.9145
4	-6.29598	-0.73361	1.9517
4	-6.29632	-0.74632	1.9692
5	-6.29644	-0.75379	1.9776

TABLE 7



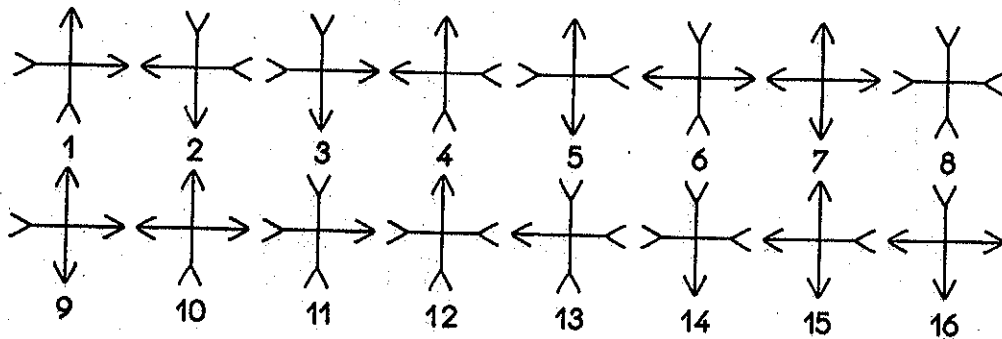


FIG. 1 - STILCK ET AL.

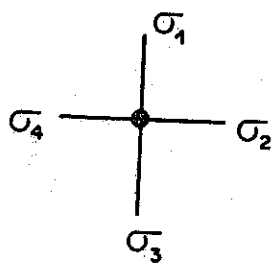


FIG. 2 - STILCK ET AL.

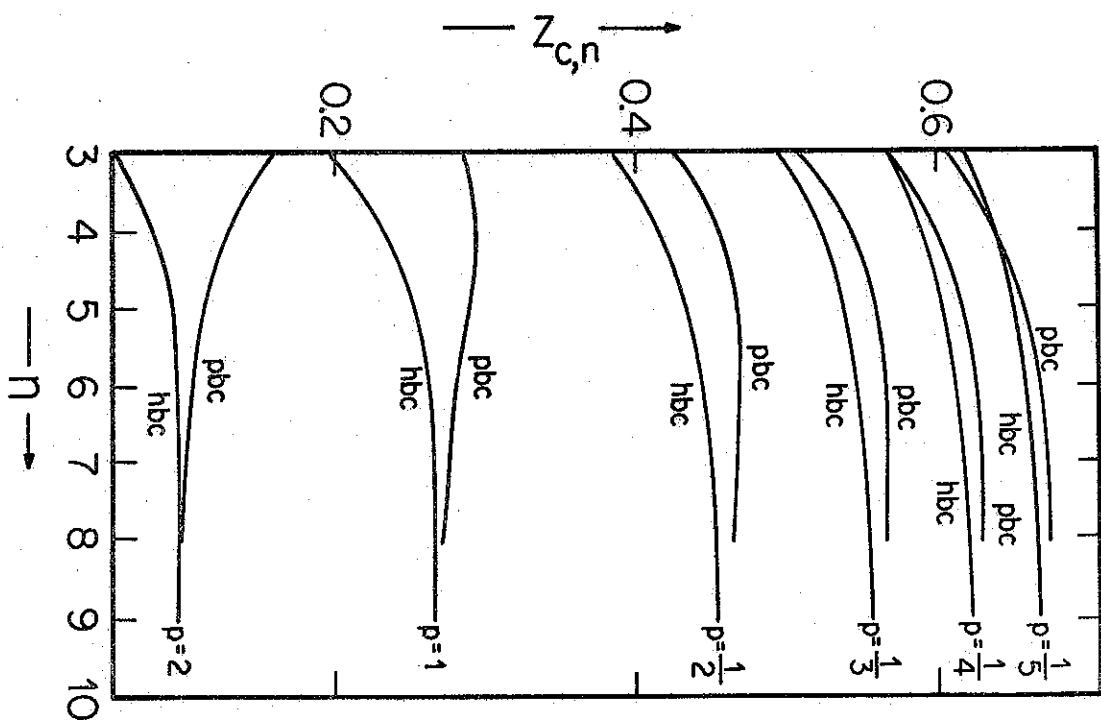


FIG. 3a - STILCK ET AL.

FIG. 3a

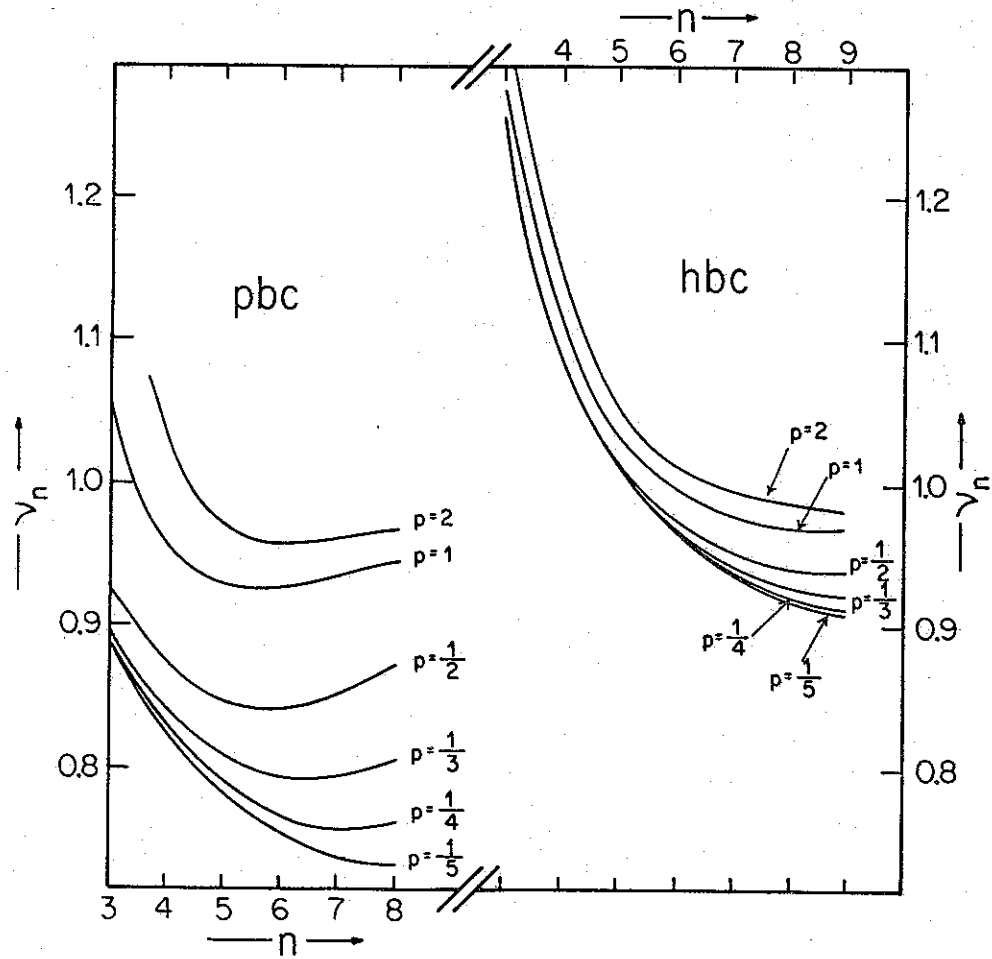


FIG. 3a - STILCK ET AL.

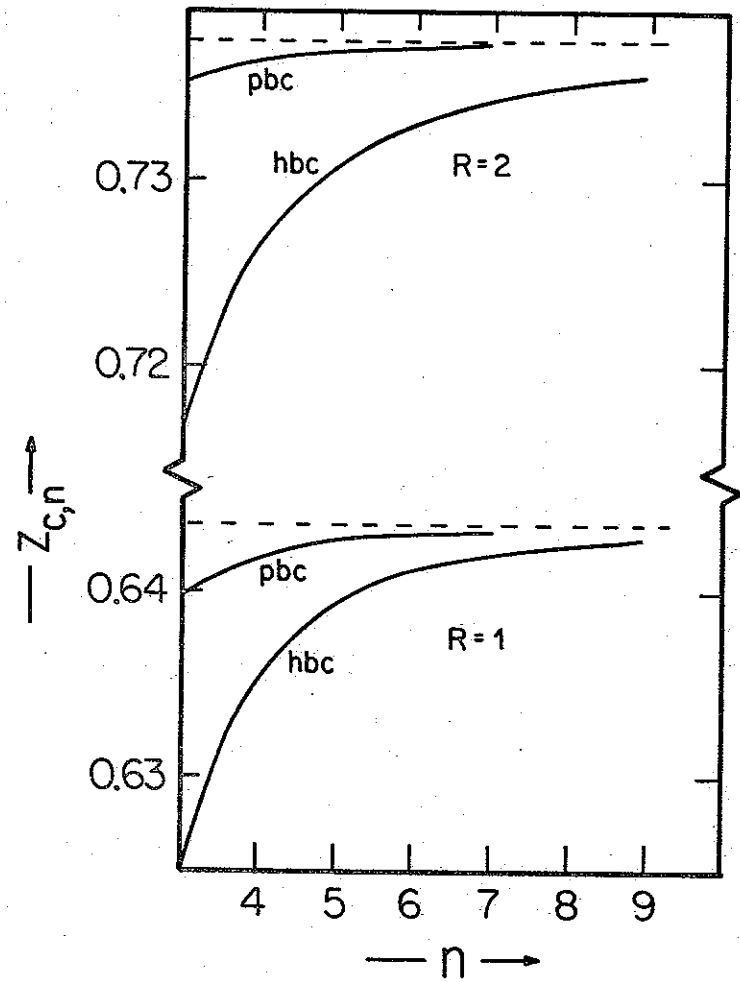


FIG. 4a - STILCK ET AL.

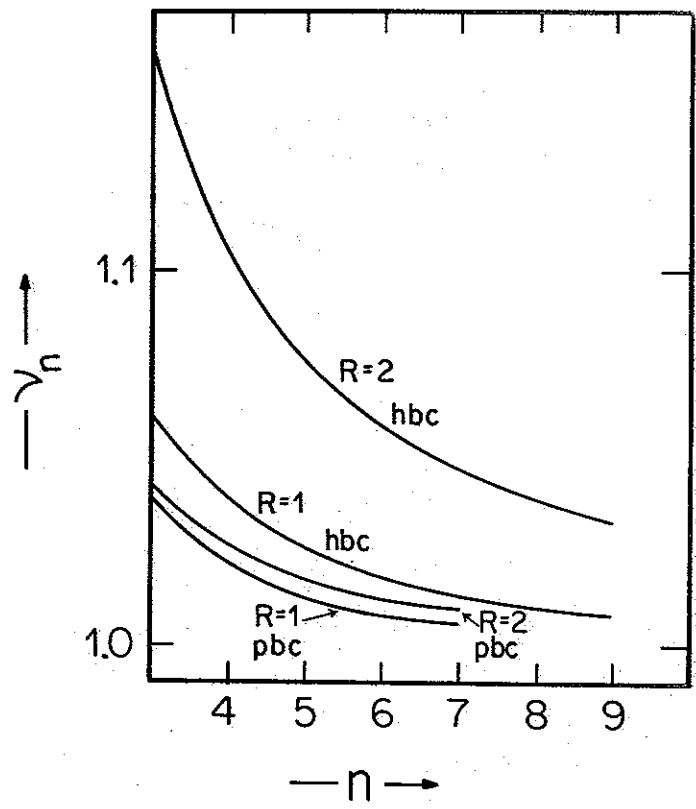


FIG. 4b - STILCK ET AL.

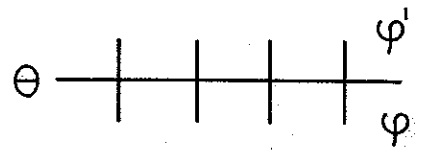


FIG. 5 - STILCK ET AL.

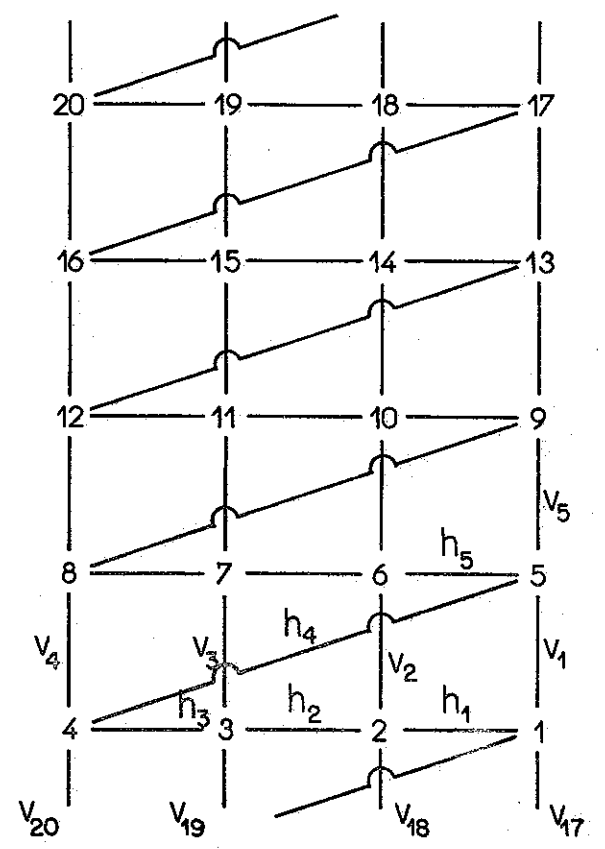


FIG. 6 - STILCK ET AL.